GEOPHYSICAL RESEARCH LETTERS, VOL. 33, L24314, doi:10.1029/2006GL027890, 2006



# Seismic imaging of deep low-velocity zone beneath the Dead Sea basin and transform fault: Implications for strain localization and crustal rigidity

Uri S. ten Brink,[1] Abdallah S. Al-Zoubi,[2] Claudia H. Flores,[3] Yair Rotstein,[3,4] Isam Qabbani,[5] Steve H Harder,[6] and G. Randy Keller[6,7]

Received 15 August 2006; revised 3 November 2006; accepted 15 November 2006; published 23 December 2006.

[1] New seismic observations from the Dead Sea basin (DSB), a large pull-apart basin along the Dead Sea transform (DST) plate boundary, show a low velocity zone extending to a depth of 18 km under the basin. The lower crust and Moho are not perturbed. These observations are incompatible with the current view of mid-crustal strength at low temperatures and with support of the basin's negative load by a rigid elastic plate. Strain softening in the middle crust is invoked to explain the isostatic compensation and the rapid subsidence of the basin during the Pleistocene. Whether the deformation is influenced by the presence of fluids and by a long history of seismic activity on the DST, and what the exact softening mechanism is, remain open questions. The uplift surrounding the DST also appears to be an upper crustal phenomenon but its relationship to a mid-crustal strength minimum is less clear. The shear deformation associated with the transform plate boundary motion appears, on the other hand, to cut throughout the entire crust. **Citation:** ten Brink, U. S., A. S. Al-Zoubi, C. H. Flores, Y. Rotstein, I. Qabbani, S. H. Harder, and G. R. Keller (2006), Seismic imaging of deep low-velocity zone beneath the Dead Sea basin and transform fault: Implications for strain localization and crustal rigidity, *Geophys. Res. Lett.*, *33*, L24314, doi:10.1029/2006GL027890.

## 1. Introduction

[2] Continental transform faults provide a simple setting in which deformation and the rheological stratification of the continental crust can be studied. These studies are important to the understanding of the long-term strength of the continental lithosphere, subsidence of sedimentary basins, and the earthquake deformation cycle. However, seismic observations of strain distribution in the continental crust beneath the San Andreas Fault provide conflicting evidence for strain localization, the depth of brittle behavior, and the existence of subhorizontal detachments [*Brocher et al.*, 1994; *Fuis et al.*, 2003; *Henstock et al.*, 1997; *Parsons and Hart*, 1999]. Unlike the San Andreas Fault, which is located over a fossil subduction zone, The DST is located at the boundary between the stable Arabian shield and its Triassic-Jurassic Tethys passive continental margin (the present eastern Mediterranean), and is free of recent thermal and mechanical inputs.

[3] We report here first results from a seismic refraction experiment across the Dead Sea basin (DSB), a large pull-apart basin along the DST, conducted during October 2004 and discuss their implications to the deformation and rheology of the continental crust. The experiment consisted of two wide-angle seismic reflection and refraction profiles: a 280-km-long profile along the international border between Jordan, Israel and the West Bank at the center of the Dead Sea rift, and a 250-km-long profile from the Gaza Strip to eastern Jordan across the Dead Sea rift. The east-west line (Figure 1a), discussed here, consisted of seismograms from 334 miniature stand-alone seismic recorders (RefTek 125, Texans), recording five inline 1-ton underground explosions. The Texans were attached to a single vertical 4.5 Hz geophone, buried, and placed at intervals of 0.65–0.75 km along the profile. The data were plotted as shot-gathers and modeled interactively using forward and inverse ray tracing routines (Figures S1 and S2 in the auxiliary material).[1] The velocity model that resulted from our analysis is shown as Figure 1b.

## 2. Interpretation of Velocity Model

[4] The velocity model is constructed as a series of layers, which are not a-priori correlated with the stratigraphy, and velocities can vary laterally within any model layer.

### 2.1. Sedimentary Section

[5] Low *P*-wave velocities in the top two model layers within the DSB (Figure 1b) are interpreted to represent Miocene and younger basin fill of mostly continental and lacustrine sediments. The thickness of these layers (6.2 km) is similar to that encountered in Sedom Deep-1 borehole nearby (6.45 km [*Gardosh et al.*, 1997]; well 3 in Figure 1a). The third model layer under the basin is considerably slower (5–5.9 km/s) than in the surrounding regions and is interpreted to be the pre-basin sedimentary rocks, which were

[1]U.S. Geological Survey, Woods Hole, Massachusetts, USA.
[2]Surveying and Geomatics Department, Al-Balqa' Applied University, Salt, Jordan.
[3]Geophysical Institute of Israel, Lod, Israel.
[4]Now at the U.S.-Israel Binational Science Foundation, Jerusalem, Israel.
[5]Natural Resources Authority, Amman, Jordan.
[6]Department of Geological Sciences, University of Texas at El Paso, El Paso, Texas, USA.
[7]Now at School of Geology and Geophysics, University of Oklahoma, Norman, Oklahoma, USA.


0094-8276/06/2006GL027890$05.00

[1]Auxiliary material data sets are available at ftp://ftp.agu.org/apend/gl/2006gl027890. Other auxiliary material files are in the HTML.

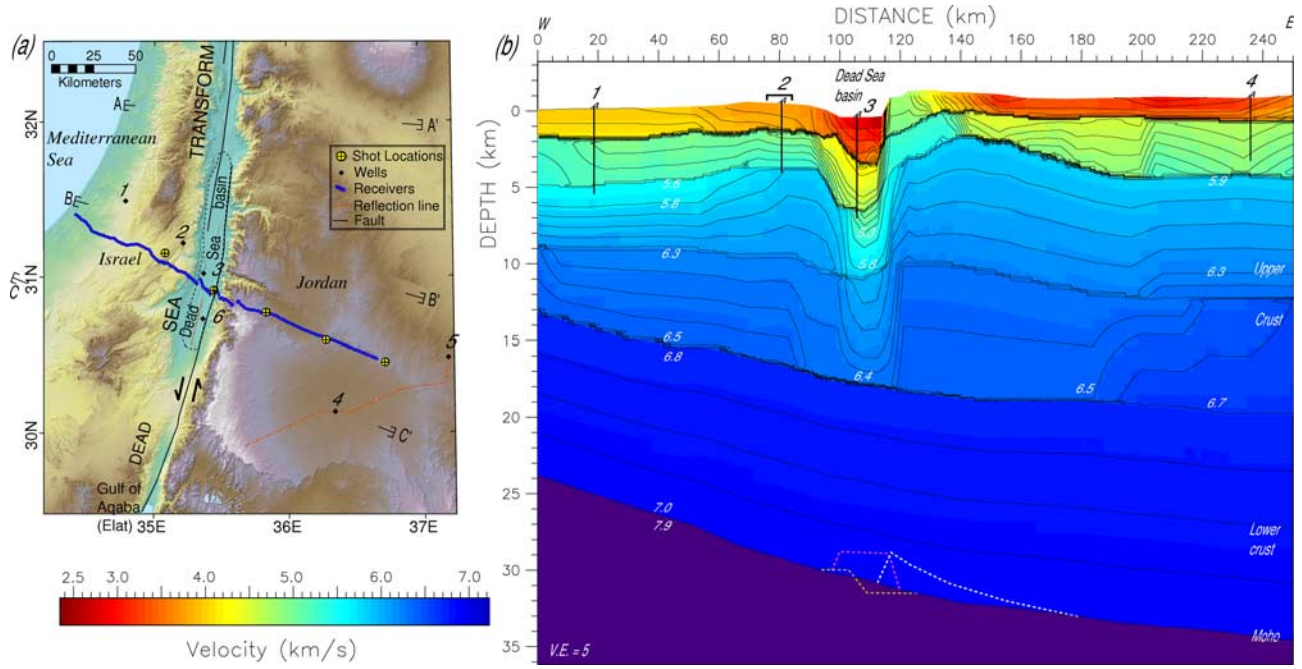


**Figure 1.** (a) Location of seismic refraction profile, deep wells, and fault system, on a shaded topographic relief map. Note the rift-like morphology of the DST. A, B, and C mark the locations of profiles in Figure 2b. (b) *P*-wave velocity model along the seismic profile. White and pink dashed lines are various perturbations to Moho topography with amplitudes that are within the data resolution. Velocity contour interval varies for clarity. Wells are marked by vertical lines. Bracket points to location of reference section. See text for further explanations.

down-dropped by the pull-apart basin. It is ~4 km thick, slightly thicker than the inferred 3 km thick pre-basin section [*Gardosh et al.*, 1997; *Gilboa et al.*, 1993], but similar in thickness to the nearly uneroded sedimentary section west of the rift valley.

[6] The upper two model layers east of the DSB represent mostly Paleozoic sedimentary layers (Figure 2a), which are dominantly sandstones. Borehole and seismic reflection data 30 km south of our profile (Figure 1a), place middle Cambrian rocks at depths of 3.5–4.5 km. The velocity of these two layers increase significantly within 25 km of the DSB due to erosion caused by transform-shoulder uplift, which brought deeper sedimentary and crystalline rocks closer to the surface. The upper two model layers of the model west of the DSB represent mostly Mesozoic sedimentary layers, which consist dominantly of carbonate rocks and therefore have higher *P*-wave velocities than east of the DSB. The sedimentary thickness increases from ~4.5 km near the DSB to ~5 km at the western end of the profile, in accord with deep boreholes in the area (Wells 1 and 2 in Figure 1).

### 2.2. Upper Crustal Section

[7] The fourth model layer under the DSB reaches 18 km depth and is interpreted as the crystalline upper crust under the basin. Its velocity is lower than the surrounding regions. Outside the DSB, the third and fourth model layers range in velocity between 5.9–6.5 km/s and represent the upper crust. The uppermost layer 3 velocity on the western end of the profile is slightly lower, 5.6 km/s, representing perhaps the infra-Cambrian Zenifim Formation of arkose and volcanic rocks above the crystalline basement. The easternmost 50 km of the profile is characterized by higher velocities, 5.9–6.8 km/s, but in the absence of additional information about crustal heterogeneities, we cannot interpret this lateral velocity change.

### 2.3. Lower Crust and Moho

[8] A lower crustal velocity gradient of 6.8–7.0 km/s is present under the entire profile and matches the inferred lower crustal composition of pyroxene and garnet granulites based on xenoliths [*McGuire and Stern*, 1993]. There is no indication for a low velocity anomaly extending into the lower crust under the DSB (see auxiliary material). Moho depth changes from 35 km at the eastern end of the profile to 30.7 km under the rift valley and 24 km at the western end of the profile. The Moho depth matches within 1 km the Moho depth in crossing refraction profiles in Jordan [*El-Isa et al.*, 1987] under the DSB, and in western Israel [*Ginzburg et al.*, 1979]. Upper mantle velocity is 7.9 km/s, similar to previous studies [*DESERT Group*, 2004], but is not well constrained.

### 2.4. Depth Resolution at the Moho

[9] A small asymmetric Moho relief with an amplitude of ~1.5 km was previously modeled under the DST 70 km to the south and was interpreted as an expression of a through-going crustal fault [*DESERT Group*, 2004]. We perturbed our best-fitting model to test possible configurations under the basin. These included a Moho step, a 20-km wide upper mantle intrusion into the lower crust, and an upward flexure of the Moho from the east toward the rift valley, which reaches shallower depth than the best-fit model (Figure 1b).

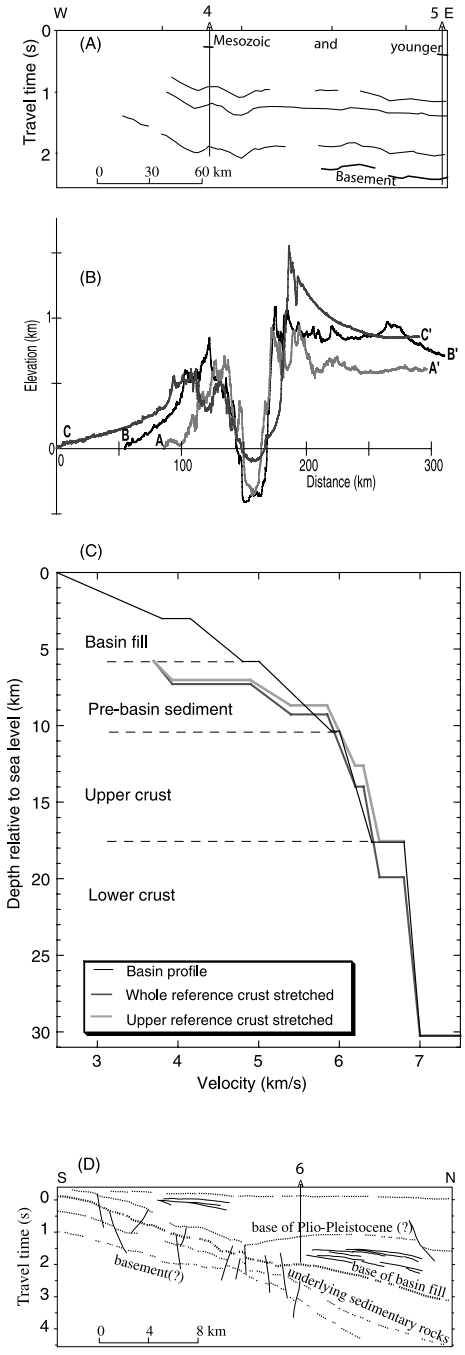


**Figure 2.** (a) Line drawing of prominent reflections in an unpublished composite deep seismic reflection profile across SE Jordan. Note the abrupt start of uplift toward the DST. See Figure 1a for location. (b) Comparison between topographic profiles across the center of the DSB (B-B′) and outside the DSB (A-A′, C-C′). See Figure 1a for profile locations. (c) Velocity gradient under the basin (thin black line) and velocity profiles of the reference section underlying bracket in Figure 1b, thinned proportionally and shifted down to the base of the basin fill. See text for discussion. (d) Line drawing interpretation of a seismic profile along the southern end of the DSB (modified from *Al-Zoubi and ten Brink* [2002]). Thin lines are prograding lacustrine(?) sequences. Note the sagging of the basin without prominent boundary faults, and the possible southward extension of the basin with time. See Figure 1a for location.

These various perturbations of Moho relief do not degrade the fit the observations considerably as long as Moho relief does not exceed 2–2.5 km (see auxiliary material).

## 3. Depth Extent of the Plate Boundary

[10] Although variations in seismic velocity under the DSB do not extend into the lower crust, the top and bottom boundaries of the lower crust do change their slopes there. This observation is robust. Perturbations to the best-fit model to create a single slope along the entire seismic profile for the upper-to-lower crust interface and for the Moho interface, result in noticeable degradation of model fit (see auxiliary material). A similar observation was inferred from gravity data north of the DSB [*ten Brink et al.*, 1990]. The observed rapid crustal thinning west of the transform fault is due to the transition from a normal continental crust to an oceanic or thinned continental crust of the eastern Mediterranean Sea across the Tethys passive continental margin [e.g., *Ginzburg et al.*, 1979]. The almost constant crustal thickness east of the transform fault reflects the fact that this section was ~107 km to the south relative to its present position before the transform fault started its motion, and was therefore farther away from the continental margin. Therefore, the changes in the slopes of upper-to-lower crustal boundary and of the Moho indicate that the plate boundary extends through the mafic lower crust, juxtaposing laterally offset crusts, although the exact width of the shear zone there cannot be determined from the data.

## 4. Isostatic Compensation and Elastic Thickness

[11] The velocity model indicates that anomalously low velocities under the DSB extend to a depth of 18 km. Because *P*-wave velocity and density are generally correlated, the sediment and upper crust under the DSB must have considerably lower density than in the surrounding highlands. Using established velocity-density relationships, the vertical stress on the lower crust (18 km depth) due to the variations in overburden is up to 45 MPa smaller under the basin than under the surrounding regions and the lateral gradient in vertical stress must be steep. (The vertical stress change is only 33 MPa, if the drop in Vp below the basin fill is caused by enhanced fluid pressure or micro-cracks, not density ([*Stern et al.*, 2001] and references therein). The vertical stress change is 57 MPa, if we use the measured densities at the 6.45 km-deep Sedom Deep well [*Rybakov et al.*, 1999] for the basin fill, instead of velocity-density relationship.) If the basin were compensated by Airy isostasy, upper mantle should have been only 15 km deep or 15.3 km above the observed Moho (for a stress difference of 45 MPa). As this is not observed, the density anomaly of the basin and the upper crust must either be supported by lithospheric rigidity or by another mechanism. Because the negative load of the basin is narrow, an elastic thickness >5 km will suffice to support the basin without a significant rise in the Moho [*ten Brink et al.*, 1993]. If the basin is supported by the flexural rigidity of the plate, the resultant horizontal tensile stresses in the upper crust should cause the Earth surface to bow up. Comparison between profiles across the center and the edges of the basin

show that this is not the case (Figure 2b), calling into question the flexural support of the basin.

[12] The morphology of the southern 930 km of the plate boundary is characterized by an uplift of an area to about 75 km on either side of the DST valley (Figure 1a). The uplift is not correlated with the location of the DSB (Figures 1a and 2b). It is most striking on the east side, where the sedimentary section is tilted away from the DST without signs of compressional tectonics, similar to other rift-flank uplifts. Previous models all assumed that the uplift involves the entire crust [*Sobolev et al.*, 2005; *ten Brink et al.*, 1990; *Wdowinski and Zilberman*, 1996]. Iso-velocity contours of the seismic velocity model (Figure 1b) indicate that uplift-related deformation is limited to the uppermost 10–15 km of the crust and the lower crust is not involved in the uplift. If the upper crustal uplift is supported by an elastic plate, the distance from the DST to the minimum deflection on the east side ($X_b$ = 75 km), is compatible with an elastic thickness between 7 km ($\alpha * \pi$) for a continuous plate and 10 km ($\alpha * 3\pi/4$) for a broken plate, where $\alpha$ is the flexural wavelength [*Turcotte and Schubert*, 1982]. A regional seismic reflection profile (Figure 2a) shows, however a kink and a linear uplift rather than the smooth curvature, as is expected for flexural support of the uplift.

## 5. Origin of the Low-Velocity Zone

[13] Pull-apart basins are generated by fault-parallel extension in areas of geometrical irregularities within strike-slip faults. As such, they represent mechanical extension of the continental crust with little contribution from external or internal heating. Heat will dissipate rapidly laterally during extension because of the narrow width of such basins [*Pitman and Andrews*, 1985; *ten Brink et al.*, 1993]. In addition, igneous activity is not known within the DSB. Therefore, the velocity structure represents the results of mechanical extension of the crust. Alternatively, deep low-velocity zone may arise from excess pore fluid pressure, as is likely the case for the Alpine Fault, New Zealand [*Stern et al.*, 2001]. The Alpine fault, however, is atypical of strike-slip faults with its high electrical conductivity, the associated thick metamorphic belt, and its dip of 40° [*Stern et al.*, 2001]. Similar deep low-velocity zone was not observed at the San Andreas fault [e.g., *Brocher et al.*, 1994; *Fuis et al.*, 2003; *Henstock et al.*, 1997; *Parsons and Hart*, 1999], with the exception of one study [*Trehu and Wheeler*, 1987], whose layout was not suitable for detection of velocity variations across the fault. A seismic refraction profile across the DST outside the basin [*DESERT Group*, 2004] shows no crustal velocity perturbations. Because the tectonic setting and crustal composition of the Alpine Fault are different from those at the DST, we interpret the observed low velocity under the DSB to the extension of the pull-apart basin, and not to velocity reduction along strike-slip faults. We follow *Gardosh et al.* [1997] and *Gilboa et al.* [1993] in considering the barely eroded crustal section 20 km west of the DSB as the reference section that approximates the crust prior to basin opening (bracket in Figure 1b). If the pull-apart basin were to form kinematically by whole-crust extension, that reference section would have had to thin to 83% of its original thickness (stretching factor, $\beta$ = 1.21) to accommodate the subsidence and filling of the Dead Sea basin (Figure 2c). In that case, upper crustal rocks with velocities <6.5 km would have extended to a depth of 20.3 km and into the surrounding lower crust. Sensitivity tests show that such an anomaly would have been detected by our data (see auxiliary material). Hence, the data does not support whole crust brittle-plastic extension and faults reaching the Moho. A brittle-plastic crust was previously proposed based on the concentration of micro-earthquake activity at depths of 20–32 km [*Aldersons et al.*, 2003], but a new double-differencing relocation study show earthquake clustering at depths of 8–10 and 12–16 km [*Shamir*, 2006]. A better relocation effort, that takes into account the highly heterogeneous velocity structure of the area, is needed.

[14] If on the other hand, the upper crust accommodates basin subsidence without lower crustal involvement, the reference upper crust would have had to thin to 67% of its original thickness ($\beta$ = 1.49). In this case, the reference upper crustal section is expected to shrink to the available space below the basin, resulting in a slightly higher than observed (but still within resolution error) upper crustal velocities (Figure 2c). Subsidence is limited to the upper crust either because the bounding faults of the pull-apart basin dip toward each other and coalesce into a single fault trace in the lower crust [*Segall and Pollard*, 1980], or because the faults terminate at a viscous layer, as was suggested for faults in southern California [*Deng et al.*, 1998]. A coalescing fault geometry requires isostatic uplift to support the negative load of the basin, which is not observed. A viscous layer above 18 km depth, on the other hand, is compatible with the lack of isostatic support for the negative load and for the observation that uplift of the areas surrounding the DST does not extend deeper than 10–15 km. The axial extension of this layer may accommodate part of the stretching and subsidence due to pull-apart opening. A near-surface evidence for such extension may be found in the sagging of the southern DSB to a depth of 5 km without significant border faults, and the possible southward elongation of the basin with time (Figure 2d) [*Al-Zoubi and ten Brink*, 2002].

## 6. Strain Distribution

[15] Viscous deformation at depths above 18 km requires a relatively high geothermal gradient [*Petrunin and Sobolev*, 2006; *ten Brink*, 2002] even for mid-crustal composition of quartz and feldspar [*McGuire and Stern*, 1993]. For example, thermo-mechanical models of the Dead Sea can generate a viscous layer only at depths greater than 25 km and with higher assumed heat flow (60 mW/m$^2$ [*Petrunin and Sobolev*, 2006]) than is observed (45–53 mW/m$^2$ [e.g., *Eckstein and Simmons*, 1978]). These models rely on extrapolations to geological conditions of experimentally determined power law creep from significantly lower strain rates and higher temperatures. They do not take into account dynamic processes that can reduce the layer strength and induce strain localization [*Regenauer-Lieb et al.*, 2006]. Various softening mechanisms have been suggested to explain the observations of exhumed middle crustal shear zones [*Gueydan et al.*, 2003] and post-seismic relaxation [*Montesi and Hirth*, 2003]. These mechanisms include shear heating, grain-size sensitive flow, and reaction softening. Grain-size sensitive flow assumes that quartzite strength decreases significantly with decrease in grain size via recrystalization, which leads to

changes in the deformation mode from dislocation creep to diffusion creep [*Montesi and Hirth*, 2003]. Reaction softening refers to pervasive transformation of feldspar within microfaults to white mica in the presence of free water [*Gueydan et al.*, 2003].

[16] Localized shear heating due to motion on the DST may sufficiently increase the temperatures to allow for ductile flow, but the starting temperatures at the relevant depths under the DSB may be too low ($\leq$300°C [*ten Brink*, 2002]). On the other hand, conditions exist for reaction softening and perhaps for grain-size reduction to occur under the DSB. Free water in the granitic and metamorphic crust can be drawn into the middle crust under the DSB by the large negative vertical stress ($\leq$45 MPa) under the basin relative to the surrounding areas. Microfracturing is facilitated by seismic activity on the DST during the $\sim$16 m.y. of strike-slip motion. These conditions may explain the accelerated subsidence of the DSB during the Pleistocene (4.4 km [*Gardosh et al.*, 1997]) as a positive feedback on strain softening. As the basin deepens via brittle deformation, it exerts less vertical stress on the underlying crust than the surrounding regions. This vertical stress differential encourages fluid flow into the crust. Increased fluid concentration combined with microfaulting at the bottom of the seismogenic zone by seismic activity along the DST, allows ductile deformation of the base of the quartzo-feldpatic crust. As the deformation proceeds, more of the deformation takes place in the ductile layer, and that layer may thicken [*Gueydan et al.*, 2003] and perhaps widen laterally, leading to more rapid subsidence and the lengthening of the basin. The expected strain rate in a 1-km-thick mid-crustal layer, necessary to compensate for the accelerated subsidence of the DSB, is $4 \times 10^{-13}$ s$^{-1}$ and the estimated viscosity of that layer due to loading of 4 km of Pleistocene sediments, is $2 \times 10^{20}$ Pa-s.

[17] This feedback subsidence mechanism, which enhances the development of mid-crustal detachments by combined microfracturing and negative vertical stress may also apply to non-transform extensional sedimentary basins, where similar conditions exist.

[18] **Acknowledgments.** Funded by USAID Middle Eastern Regional Cooperation Program grant M21-012, with matching funds by the particpating institutions. We thank D. Simpson and J. Fowler, IRIS, and the Jordanian Army for their administrative and logistical support, T. Meckel, G. Kaip, M. Averill, J. Song, and M. Arsenault for their field and processing support; and the Jordanian field assistants and security personnel, for working long hours in scorching heat during the Fast of Ramadan. Discussions with E. Burov, L. Montesi, and R. Buck, and reviews by C. Ruppel, T. Parsons, G. Shamir, and T. Stern are gratefully acknowledged.

## References

Aldersons, F., Z. Ben-Avraham, A. Hofstetter, E. Kissling, and T. Al-Yazjeen (2003), Lower-crustal strength under the Dead Sea basin from local earthquake data and rheological modeling, *Earth Planet. Sci. Lett.*, *214*, 129–142.

Al-Zoubi, A., and U. S. ten Brink (2002), Lower crustal flow and the role of shear in basin subsidence: An example from the Dead Sea basin, *Earth Planet. Sci. Lett.*, *199*, 67–79, (Corrigendum, *Earth Planet. Sci. Lett.*, *201*, 447–448, 2002.)

Brocher, T. M., J. McCarthy, P. E. Hart, W. S. Holbrook, K. P. Furlong, T. V. McEvilly, J. A. Hole, and S. L. Klemperer (1994), Seismic evidence for a lower-crustal detachment beneath San Francisco Bay, California, *Science*, *265*, 1436–1439.

Deng, J., M. Gurnis, H. Kanamori, and E. Hauksson (1998), Viscoelastic flow in the lower crust after the 1992 Landers, California, earthquake, *Science*, *282*, 1689–1692.

DESERT Group (2004), The crustal structure of the Dead Sea transform, *Geophys. J. Int.*, *156*, 655–681.

Eckstein, Y., and G. Simmons (1978), Measurements and interpretation of terrestrial heat flow in Israel, *Geothermics*, *6*, 117–142.

El-Isa, Z. H., J. Mechie, C. Prodehl, J. Makris, and R. Rihm (1987), A crustal structure study of Jordan derived from seismic refraction data, *Tectonophysics*, *138*, 235–253.

Fuis, G. S., et al. (2003), Fault systems of the 1971 San Fernando and 1994 Northridge earthquakes, southern California: Relocated aftershocks and seismic images from LARSE II, *Geology*, *31*, 171–174.

Gardosh, M., E. Kashai, S. Salhov, H. Shulman, and E. Tannenbaum (1997), Hydrocarbon exploration in the southern Dead Sea basin, in *The Dead Sea: The Lake and Its Setting*, edited by T. M. Niemi et al., pp. 57–72, Oxford Univ. Press, New York.

Gilboa, Y., H. Fligelman, B. Derin, N. H. Foster, and E. A. Beaumont (1993), Zohar-Kidod-Haqanaim fields: Israel, eastern Mediterranean basin, in *Structural Traps*, vol. 8, *Treatise of Petroleum Geology Atlas of Oil and Gas Fields*, edited by N. H. Foster and E. A. Beaumont, pp. 129–152, Am. Assoc. of Pet. Geol., Tulsa, Okla.

Ginzburg, A., J. Makris, K. Fuchs, C. Prodehl, W. Kaminski, and U. Amitai (1979), A seismic study of the crust and upper mantle of the Jordan-Dead Sea rift and their transition toward the Mediterranean Sea, *J. Geophys. Res.*, *84*, 1569–1582.

Gueydan, F., Y. M. Leroy, L. Jolivet, and P. Agard (2003), Analysis of continental midcrustal strain localization induced by microfracturing and reaction-softening, *J. Geophys. Res.*, *108*(B2), 2064, doi:10.1029/2001JB000611.

Henstock, T. J., A. Levander, and J. A. Hole (1997), Deformation in the lower crust of the San Andreas fault system in northern California, *Science*, *278*, 650–653.

McGuire, A. V., and R. J. Stern (1993), Granulite xenoliths from western Saudi Arabia: The lower crust of the late Precambrian Arabian-Nubian shield, *Contrib. Mineral. Petrol.*, *114*, 395–408.

Montesi, L. G. J., and G. Hirth (2003), Grain size evolution and the rheology of ductile shear zones: From laboratory experiments to postseismic creep, *Earth Planet. Sci. Lett.*, *211*, 97–110.

Parsons, T., and P. E. Hart (1999), Dipping San Andreas and Hayward faults revealed beneath San Francisco Bay, California, *Geology*, *27*, 839–842.

Petrunin, A., and S. V. Sobolev (2006), What controls thickness of sediments and lithospheric deformation at a pull-apart basin?, *Geology*, *34*, 389–392.

Pitman, W. C., III, and J. A. Andrews (1985), Subsidence and thermal history of small pull-apart basins, *Spec. Publ. Soc. Econ. Paleontol. Mineral.*, *37*, 45–119.

Regenauer-Lieb, K., R. F. Weinberg, and G. Rosenbaum (2006), The effect of energy feedbacks on continental strength, *Nature*, *442*, 67–70.

Rybakov, M., V. Goldshmidt, Y. Rotstein, L. Fleischer, I. Goldberg, C. Campbell, and P. Millegan (1999), Petrophysical constraints on gravity/magnetic interpretation in Israel, *Leading Edge*, *18*, 269–272.

Segall, P., and D. D. Pollard (1980), Mechanics of discontinuous faults, *J. Geophys. Res.*, *85*, 4337–4350.

Shamir, G. (2006), The active structure of the Dead Sea depression, *Spec. Pap. Geol. Soc. Am.*, *401*, 15–32.

Sobolev, S. V., A. Petrunin, Z. Garfunkel, and A. Babeyko (2005), Thermomechanical model of the Dead Sea transform, *Earth Planet. Sci. Lett.*, *238*, 78–95.

Stern, T. A., S. Kleffman, D. A. Okaya, M. Scherwath, and S. Bannister (2001), Low seismic-wave speeds and enhanced fluid pressure beneath the Southern Alps of New Zealand, *Geology*, *29*, 679–682.

ten Brink, U. S. (2002), Corrigendum to 'Lower crustal flow and the role of shear in basin subsidence: An example from the Dead Sea Basin' [Earth Planet. Sci. Lett. 199 (2002) 67–79], *Earth Planet. Sci. Lett.*, *201*, 447–448.

ten Brink, U. S., N. Schoenberg, R. L. Kovach, and Z. Ben-Avraham (1990), Uplift and a possible Moho offset across the Dead Sea transform, *Tectonophysics*, *180*, 71–85.

ten Brink, U. S., Z. Ben-Avraham, R. E. Bell, M. Hassouneh, D. F. Coleman, G. Andeasen, G. Tibor, and B. Coakley (1993), Structure of the Dead Sea pull-apart basin from gravity analysis, *J. Geophys. Res.*, *98*, 21,887–21,894.

Trehu, A. M., and W. H. I. Wheeler (1987), Possible evidence for subducted sedimentary materials beneath central California, *Geology*, *15*, 254–258.

Turcotte, D. L., and G. Schubert (1982), *Geodynamics Applications of Continuum Physics to Geological Problems*, John Wiley, Hoboken, N. J.

Wdowinski, S., and E. Zilberman (1996), Kinematic modelling of large-scale structural asymmetry across the Dead Sea rift, *Tectonophysics*, *266*, 187–201.

A. S. Al-Zoubi, Surveying and Geomatics Department, Al-Balqa' Applied University, Salt, 19117 Jordan.

C. H. Flores and U. S. ten Brink, U.S. Geological Survey, 384 Woods Hole Road, Woods Hole, MA 02543, USA. (utenbrink@usgs.gov)

S. H. Harder, Department of Geological Sciences, University of Texas at El Paso, 500 W. University Avenue, El Paso, TX 79968, USA.

G. R. Keller, School of Geology and Geophysics, University of Oklahoma, 100 East Boyd Street, Suite 810, Norman, OK 73019, USA.

I. Qabbani, Natural Resources Authority, P.O. Box 7, Amman, 11118 Jordan.

Y. Rotstein, U.S.-Israel Binational Science Foundation, 2 Alharizi Street, P.O. Box 7677, Jerusalem 91076, Israel.